

## Guidelines for the design of appropriate structures for proper capacitance-voltage measurements on III–V quantum wells

Siddhartha Panda and Dipankar Biswas

Citation: *Journal of Applied Physics* **108**, 066104 (2010); doi: 10.1063/1.3462395

View online: <http://dx.doi.org/10.1063/1.3462395>

View Table of Contents: <http://scitation.aip.org/content/aip/journal/jap/108/6?ver=pdfcov>

Published by the [AIP Publishing](#)

---



## Re-register for Table of Content Alerts

Create a profile.



Sign up today!



## Guidelines for the design of appropriate structures for proper capacitance-voltage measurements on III–V quantum wells

Siddhartha Panda<sup>a)</sup> and Dipankar Biswas

*Institute of Radiophysics and Electronics, University of Calcutta, 92 A. P. C. Rd., Kolkata 700009, India*

(Received 22 March 2010; accepted 8 June 2010; published online 28 September 2010)

Errors encountered in the capacitance-voltage ( $C$ - $V$ ) measurements of quantum well (QW) structures are usually attributed to Debye smearing. The other sources from which errors may occur are not well discussed in literature. In this paper we have highlighted the limits of  $C$ - $V$  measurements on QW structures. Simulations have been carried out through the self-consistent solutions of the Schrödinger and Poisson equations for various band offsets, dopings, and temperatures. This will provide guidelines for suitable design of quantum structures for proper  $C$ - $V$  measurements. © 2010 American Institute of Physics. [doi:10.1063/1.3462395]

The capacitance-voltage ( $C$ - $V$ ) technique is one of the most widely used nondestructive methods for determining the carrier distribution in nanostructures.<sup>1,2</sup> The deep level transient spectroscopy and the photocapacitance measurements, other versions of the  $C$ - $V$  technique, are extensively used to characterize deep levels, interface states and band offsets of strained and unstrained quantum wells (QWs).<sup>3–5</sup>

The typical structure used for  $C$ - $V$  measurements consists of a properly formed Schottky barrier on the top of the grown semiconductor and an ohmic contact at the bottom of the substrate. One or more QWs are sandwiched in the bulk semiconductor.

For proper and accurate measurements on a QW the depth of the QW from the Schottky is of utmost importance. Various research groups have developed their own models for calculation of the depth of the QW from  $C$ - $V$  measurements where the difference between the actual depth and the experimental depth is often quite large, even to the extent of 50 nm.<sup>6</sup> Although a lot of work has been carried out in the  $C$ - $V$  technique, its limitations leading to errors have not been discussed in detail excepting for the effect of Debye smearing.

The design of the QW structure should be done following the two extremely necessary conditions. On one end the QW should have a minimum distance from the Schottky, so that initially without any reverse bias the space-charge region of the Schottky junction does not enter the QW, to disturb the carrier distribution inside the well. On the other end the QW should not be too far from the Schottky so that field break down occurs before the field crosses the QW to deplete it. From these two limitations we can define the minimum and the maximum depth of the QW for a particular structure to be used in  $C$ - $V$  measurements.

In this paper we have discussed in detail the design of proper quantum structures for different doping levels and different band offsets at different temperatures considering model single QW structures. The Schrödinger and Poisson equations have been solved self-consistently which is a must to determine the carrier profile of the QW structure.

In our study we consider a model Schottky structure containing a single QW sandwiched in  $n$ -doped bulk semiconductor. The metal of the Schottky barrier is Au.

The one-dimensional Schrödinger equation can be written as

$$-\frac{\hbar}{2} \frac{d}{dz} \left( \frac{1}{m^*(z)} \frac{d\psi(z)}{dz} \right) + V(z)\psi(z) = E\psi(z), \quad (1)$$

where  $\psi$  is the wave function,  $E$  is the energy eigenvalue,  $m^*$  is the electron effective mass, and  $V$  is the potential energy. As proposed by Tan *et al.*,<sup>7</sup> Eq. (1) can be discretized using the finite difference method with a uniform mesh size  $h$  as

$$-\frac{\hbar^2}{2} \left( \frac{\psi_{i+1} - \psi_i}{m_{i+1/2} h^2} - \frac{\psi_i - \psi_{i-1}}{m_{i-1/2} h^2} \right) + V_i \psi_i = E \psi_i, \quad (2)$$

and modified to a matrix eigenvalue equation

$$H\psi = E\psi, \quad (3)$$

where  $H$  is a tridiagonal symmetric matrix.

The one-dimensional Poisson equation is given by

$$\frac{d}{dz} \left( \varepsilon(z) \frac{d\varphi(z)}{dz} \right) = -q[N_D^+(z) - n(z)], \quad (4)$$

where  $\varphi$  is the electrostatic potential,  $\varepsilon$  is the coordinate dependent dielectric constant,  $N_D^+$  is the ionized donor concentration, and  $n$  is the electron concentration in the conduction band. The electron concentration in the QW region is calculated from the expression,<sup>8</sup>

$$n(z) = \frac{m^*(z)kT}{\pi\hbar^2} \sum_i \ln \left[ 1 + \exp \left( \frac{E_F - E_i}{kT} \right) \right] |\psi_i(z)|^2, \quad (5)$$

where  $E_F$  is the Fermi level,  $E_i$  is the  $i$ th bound state in the well, and  $\psi_i$  is the corresponding normalized wave function which are obtained by solving Eq. (1). Outside the QW region the electron concentration is computed through the Fermi integral as

<sup>a)</sup>Electronic mail: siddhartha.panda.2@gmail.com.

$$= N_c F_{1/2} \left( \frac{E_F - V(z)}{kT} \right), \quad (6)$$

where  $N_c$  is the effective density of state in the conduction band and  $V$  is the potential energy which is considered to be equal to the bottom of the conduction band and defined as

$$V(z) = -q\varphi(z) + \Delta E_c, \quad \text{inside QW}, \\ = -q\varphi(z), \quad \text{outside QW}, \quad (7)$$

where  $\Delta E_c$  is the band offset of the conduction band.

Equation (4) is also discretized as Schrödinger equation,

$$\left( \frac{\varepsilon_{i+1/2}(\varphi_{i+1} - \varphi_i)}{h^2} - \frac{\varepsilon_{i-1/2}(\varphi_i - \varphi_{i-1})}{h^2} \right) + q[N_{Di}^+ - n_i] = 0. \quad (8)$$

Equation (8) can be solved by Newton–Raphson method using the well-known matrix equation,

$$J\delta\varphi = -f(\varphi^0), \quad (9)$$

where  $J$  is the Jacobian matrix which can be expressed as

$$J_{ii} = \frac{\varepsilon_{i+1/2}}{h^2} \quad \text{if } j = i + 1, \\ = \frac{\varepsilon_{i-1/2}}{h^2} \quad \text{if } j = i - 1, \\ = -J_{ii-1} - J_{ii+1} + q \frac{\partial [N_{Di}^+ - n_i]}{\partial \varphi_i} \quad \text{if } j = i, \\ = 0 \quad \text{otherwise}, \quad (10)$$

$\delta\varphi$  is the correction vector to the initial approximation vector  $\varphi^0$  to obtain the actual vector  $\varphi$  and  $f$  is given by

$$f_i = \left( \frac{\varepsilon_{i+1/2}(\varphi_{i+1} - \varphi_i)}{h^2} - \frac{\varepsilon_{i-1/2}(\varphi_i - \varphi_{i-1})}{h^2} \right) + q[N_{Di}^+ - n_i]. \quad (11)$$

Since each iteration of the Newton–Raphson method requires the solution of the Schrödinger equation, the ultimate results satisfy the self-consistency of the two equations.

In our calculation the Fermi level in the metal is considered as the zero energy level. To solve the Poisson equation boundary conditions are at the surface,  $\varphi = \varphi_B$  and in the neutral region  $\varphi = \varphi_C$ , where  $\varphi_B$  is the Schottky barrier height and  $\varphi_C$  is the value of potential corresponding to the energy at the bottom of the conduction band. In the finite difference method the mesh size ( $h$ ) is considered 8 Å as an optimum size.

Figure 1 shows the variation in the two-dimensional (2D) electron concentration ( $n_{2D}$ ) with the external reverse bias ( $V_r$ ) in a 10 nm GaAs/InGaAs QW under  $C$ - $V$  measurements for different depths of the well from the Schottky, considering  $N_D^+ = 6 \times 10^{16} / \text{cm}^3$ ,  $\Delta E_c = 0.16$  eV, and  $T = 300$  K. It is evident from the figure that with out any applied reverse bias the QW situated at a distance of 100 nm from the Schottky is almost depleted. As the distance in-

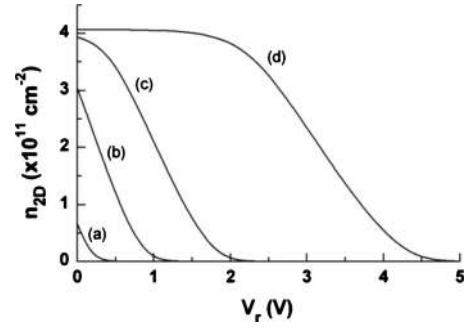


FIG. 1. Variation in the 2D electron concentration ( $n_{2D}$ ) with the external reverse bias ( $V_r$ ) in a 10 nm GaAs/InGaAs QW for the depths (a) 100 nm, (b) 150 nm, (c) 200 nm, and (d) 300 nm, considering  $N_D^+ = 6 \times 10^{16} \text{ cm}^{-3}$ ,  $\Delta E_c = 0.16$  eV, and  $T = 300$  K.

creases the depletion of the QW decreases and carriers in the QW remain unperturbed for a depth of 300 nm. So the  $C$ - $V$  profile supplies wrong information about the position of the QW and the carrier profile of the structure if the QW is not situated at a sufficient distance from the Schottky. This may be seen clearly in the experimental  $C$ - $V$  profile on multiple QWs of Yamamoto *et al.*<sup>1</sup> The first three of the eight QWs are depleted and the adjacent QWs are partially depleted.

The field distribution in the QW and in the barrier for different depths of the QW is illustrated in Fig. 2. The vertical dotted lines indicate the positions of the centers of the QWs. As shown in the figure, when the depth is 150 nm (a) the QW is depleted by the built in field. The minimum necessary depth is 368 nm (b) for proper measurements below which the QW is partially depleted. At this depth when the well is depleted the surface field is  $3.7 \times 10^5$  V/cm (c). When the depth is 404 nm (d) the well can be depleted for measurements but the surface field is almost on the verge of break down ( $\sim 4 \times 10^5$  V/cm).<sup>9</sup> For a depth of 650 nm (e) the surface field crosses break down but the field does not reach the QW. So it is cleared that for proper  $C$ - $V$  measurements the depth of the QW for the parameters mentioned should lie in the range of 368–404 nm.

Figure 3 shows the variation in the maximum and minimum depth with the ionized donor concentration at  $T = 300$  K and  $T = 50$  K for three different QW structures,  $\text{In}_{0.2}\text{Ga}_{0.8}\text{As}/\text{GaAs}$ ,  $\text{In}_{0.2}\text{Ga}_{0.8}\text{As}/\text{Al}_{0.12}\text{Ga}_{0.88}\text{As}$ , and  $\text{In}_{0.2}\text{Ga}_{0.8}\text{As}/\text{Al}_{0.35}\text{Ga}_{0.65}\text{As}$  where  $\Delta E_c$  gradually in-

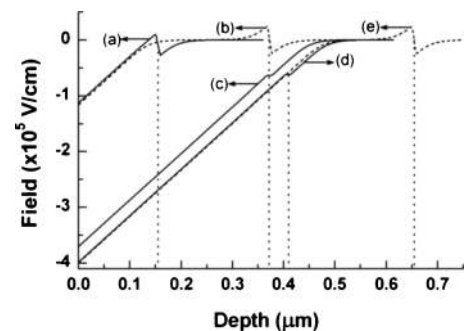


FIG. 2. Field distribution in the GaAs/InGaAs QW structure for wells at different depths, (a) 150 nm, (b) and (c) 368 nm, (d) 404 nm, and (e) 650 nm, considering  $N_D^+ = 6 \times 10^{16} \text{ cm}^{-3}$ ,  $\Delta E_c = 0.16$  eV,  $T = 300$  K, and well width = 10 nm. Vertical dotted lines indicate the positions of the centers of the QWs.

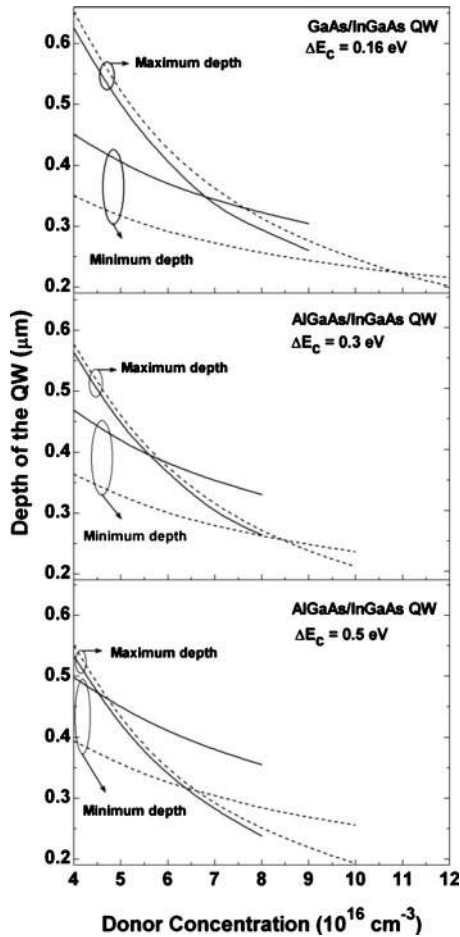


FIG. 3. Variation in the maximum and minimum depth with the ionized donor concentration for three different QW structures corresponding to different band offsets at  $T=300$  K (solid lines) and  $T=50$  K (dashed lines), considering the well width 10 nm.

creases. Details of materials and parameters used in the simulation are given in the Table I. The order of the breakdown field of Schottky barriers on GaAs and AlGaAs have been taken from standard references.<sup>9–11</sup> It is seen from the figure that, for a particular temperature, as the doping increases both the maximum and minimum distances decrease. But the maximum distance decreases more rapidly. So we obtain a critical value of doping concentration above which  $C$ - $V$  measurements lead to inaccuracies. This critical limit extends as the temperature decreases. So for the  $C$ - $V$  mea-

TABLE I. Structures and parameters used for the simulation. ( $m_0$  and  $\epsilon_0$  are the rest mass of electron and the permittivity of free space, respectively.)

QW structure	$\Delta E_C$ (eV)	$m^*/m_0$		$\epsilon/\epsilon_0$	
		Well <sup>c</sup>	Barrier <sup>d</sup>	Well <sup>e</sup>	Barrier <sup>d</sup>
$\text{In}_{0.2}\text{Ga}_{0.8}\text{As}/\text{GaAs}$	0.16 <sup>a</sup>	0.055	0.067	13.46	13.18
$\text{In}_{0.2}\text{Ga}_{0.8}\text{As}/\text{Al}_{0.12}\text{Ga}_{0.88}\text{As}$	0.3 <sup>b</sup>	0.055	0.077	13.46	12.81
$\text{In}_{0.2}\text{Ga}_{0.8}\text{As}/\text{Al}_{0.35}\text{Ga}_{0.65}\text{As}$	0.5 <sup>b</sup>	0.055	0.096	13.46	12.09

<sup>a</sup>Reference 12.

<sup>b</sup>Calculated with the help of Refs. 13, 14, and 3.

<sup>c</sup>Reference 15.

<sup>d</sup>Reference 13.

<sup>e</sup>Reference 16.

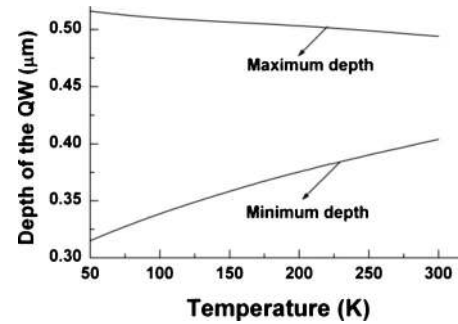


FIG. 4. Maximum and minimum depth as a function of temperature in a GaAs/InGaAs QW structure with  $N_D^+ = 5 \times 10^{16} \text{ cm}^{-3}$ ,  $\Delta E_C = 0.16 \text{ eV}$ , and well width = 10 nm.

surement of heavily doped structures, low temperature should be preferable. It should be noted that as the band offset increases this critical value of the doping concentration decreases.

The temperature dependence of the minimum and the maximum depth is presented in Fig. 4. At higher temperature the minimum depth becomes larger because of the spreading of the depletions over a wider region. On the other hand the change in the maximum depth with temperature is small.

It is worth mentioning that the simulation technique used in this work can be applied for a multiple QW structure without further modification.

In summary reports on  $C$ - $V$  measurements on single and multiple QWs for experimental determination of the position of the QW and the carrier distribution in and around the QW are often accompanied with anomalies. The errors are usually attributed to Debye smearing but other aspects of the growth and measurements from which errors may arise are not well discussed in literature. In this paper we have solve the Schrödinger and Poisson equations self-consistently to set up guide lines for the proper design of the nanostructures for  $C$ - $V$  measurements.

<sup>1</sup>N. Yamamoto, K. Yokoyama, and M. Yamamoto, *Appl. Phys. Lett.* **62**, 252 (1993).

<sup>2</sup>H. Kroemer, W. Y. Chien, J. S. Harris, Jr., and D. D. Edwall, *Appl. Phys. Lett.* **36**, 295 (1980).

<sup>3</sup>N. Debbar, D. Biswas, and P. Bhattacharya, *Phys. Rev. B* **40**, 1058 (1989).

<sup>4</sup>D. Biswas, N. Debbar, M. Razeghi, M. Defour, and F. Omnes, *Appl. Phys. Lett.* **56**, 833 (1990).

<sup>5</sup>A. V. Gelatos, J. D. Cohen, and J. P. Harbison, *Appl. Phys. Lett.* **49**, 722 (1986).

<sup>6</sup>J. B. Wang, F. Lu, S. K. Zhang, B. Zhang, D. W. Gong, H. H. Sun, and X. Wang, *Phys. Rev. B* **54**, 7979 (1996).

<sup>7</sup>I.-H. Tan, G. L. Snider, L. D. Chang, and E. L. Hu, *J. Appl. Phys.* **68**, 4071 (1990).

<sup>8</sup>P. N. Brounkov, T. Benyattou, and G. Guillot, *J. Appl. Phys.* **80**, 864 (1996).

<sup>9</sup>M. K. Hudait and S. B. Krupanidhi, *Solid-State Electron.* **43**, 2135 (1999).  
[www.ioffe.ru/SVA/NSM/Semicond/AlGaAs/basic.html](http://www.ioffe.ru/SVA/NSM/Semicond/AlGaAs/basic.html)

<sup>10</sup>F. Ma, G. Karve, X. Zheng, X. Sun, A. L. Holmes, Jr., and J. C. Campbell, *Appl. Phys. Lett.* **81**, 1908 (2002).

<sup>11</sup>V. I. Zubkov, M. A. Melnik, A. V. Solomonov, E. O. Tsvelev, F. Bugge, M. Weyers, and G. Tränkle, *Phys. Rev. B* **70**, 075312 (2004).

<sup>12</sup>S. Adachi, *J. Appl. Phys.* **58**, R1 (1985).

<sup>13</sup>*Semiconductors Group IV Elements and III-V Compounds*, edited by O. Madelung (Springer-Verlag, Berlin, 1991).

<sup>14</sup>J. C. Fan and Y. F. Chen, *J. Appl. Phys.* **80**, 6761 (1996).

<sup>15</sup>S. Adachi, *Physical Properties of III-V Semiconductor Compounds* (Wiley, New York, 1992).